PROCEEDINGS OF SCIENCE

Measurements of Higgs boson production and properties in the ZZ decay channel using the CMS detector

Simon REGNARD*†
École polytechnique / CNRS-IN2P3, Palaiseau, France
E-mail: simon.regnard@cern.ch

Measurements of Higgs boson properties using the $H \to ZZ \to 4\ell$ ($\ell = e, \mu$) decay channel are presented, based on a data sample corresponding to an integrated luminosity of 12.9 fb^{-1} of pp collisions at a center-of-mass energy of 13 TeV collected by the CMS experiment at the LHC during 2016. The observed significance for the standard model Higgs boson is 6.2σ at a mass of $m_H = 125.09$ GeV, where the expected significance is 6.5σ. The signal strength μ, defined as the ratio of the Higgs boson production cross section times branching fraction to four leptons to the standard model expectation, is measured to be $\mu = 0.99^{+0.33}_{-0.26}$. Individual strength parameters for four Higgs boson production modes are constrained for the first time using this channel. The Higgs boson mass is measured to be $m_H = 124.50^{+0.48}_{-0.46}$ GeV. The model-independent fiducial cross section is measured to be $2.29^{+0.74}_{-0.64}(\text{stat.})^{+0.30}_{-0.23}(\text{sys.})^{+0.01}_{-0.05}(\text{model dep.})$ fb, and differential cross sections as a function of the transverse momentum of the Higgs boson and the number of associated jets are measured.

38th International Conference on High Energy Physics
3-10 August 2016
Chicago, USA

*Speaker.
†on behalf of the CMS Collaboration

PoS(ICHEP2016)387

1. Introduction

Properties of the boson discovered by the CMS and ATLAS experiments at the Large Hadron Collider (LHC) in 2012 have been extensively studied with the full Run I data sample, so far confirming it as consistent with expectations for a standard model (SM) Higgs boson [1] (and references therein), while its mass was measured to be 125.09 ± 0.24 GeV from a combined CMS and ATLAS analysis [2]. The decay channel to four leptons ($\mathrm{H} \to \mathrm{ZZ} \to 4\ell$, $\ell = \mathrm{e}, \mu$) has played a crucial role in these measurements [3, 4] thanks to its large signal-to-background ratio and to the complete reconstruction of the final state products with excellent momentum resolution. After a two-year shutdown, Run II of the LHC has started in 2015 with an increased center-of-mass energy of $\sqrt{s} = 13$ TeV and instantaneous luminosities growing beyond design, allowing for new precisions tests. Using 2015 data, CMS has reported the first evidence and property measurements of the Higgs boson in the 4ℓ decay channel at the new energy [5]. This study is hereby extended by a larger set of measurements [6], now exploiting the data sample collected by CMS in the beginning of 2016, which corresponds to an integrated luminosity of 12.9 fb^{-1}.

2. Analysis strategy

The strategy for the extraction of the $\mathrm{H} \to 4\ell$ signal primarily relies on ensuring a large efficiency of reconstructing and selecting leptons. Electrons (muons) are reconstructed within the geometrical acceptance defined by $|\eta| < 2.5(2.4)$ and for transverse momenta $p_{\mathrm{T}} > 7(5)$ GeV. The scale and resolution of lepton momenta are calibrated in bins of p_{T} and η exploiting known dilepton resonances. Electron identification uses a revised multivariate discriminant which includes observables sensitive to the presence of bremsstrahlung along the electron trajectory, the shape of the electromagnetic shower, and the geometrical and momentum-energy matching between the electron supercluster and track. Non-prompt or misidentified leptons are suppressed by impact parameter requirements and by a cut on Particle-flow isolation, which is corrected for the contribution of energy deposits from pileup interactions. Possible photons from final-state radiation are recovered on a per-lepton basis and are excluded from isolation computations. Efficiencies are measured in simulation and data with the Tag-and-Probe method, in order to correct the expectations from simulated samples for possible mismodeling effects.

Four-lepton candidates are built out of two pairs of opposite-sign, same-flavor selected leptons, and are selected with a set of kinematic requirements that enhance the purity of the Higgs boson signal. When more than one 4ℓ candidate is selected, a new arbitration procedure is used, based on the best value of a matrix-element (ME) discriminant $\mathscr{D}^{\mathrm{kin}}_{\mathrm{bkg}}$ that encodes the kinematic configuration of the $\mathrm{H} \to 4\ell$ decay. In order to improve the sensitivity to the Higgs boson production mechanisms, the selected events are classified into six mutually exclusive categories, the composition of which is shown in Fig. 1. Category definitions exploit the multiplicity of jets, b-tagged jets and additional selected leptons, and requirements on four other ME discriminants. The latter are sensitive to the topologies of VBF signal events where either one or two associated jets are reconstructed and selected, and of WH and ZH events where the associated boson decays to a pair of jets.

Irreducible backgrounds to the $\mathrm{H} \to 4\ell$ signal arise from ZZ pair production via $\mathrm{q\bar{q}}$ annihilation ($\mathrm{q\bar{q}} \to \mathrm{ZZ}$) or gluon fusion ($\mathrm{gg} \to \mathrm{ZZ}$), and are estimated using simulation, whereby K-factors are applied to account for missing higher-order corrections. Reducible backgrounds arising from the

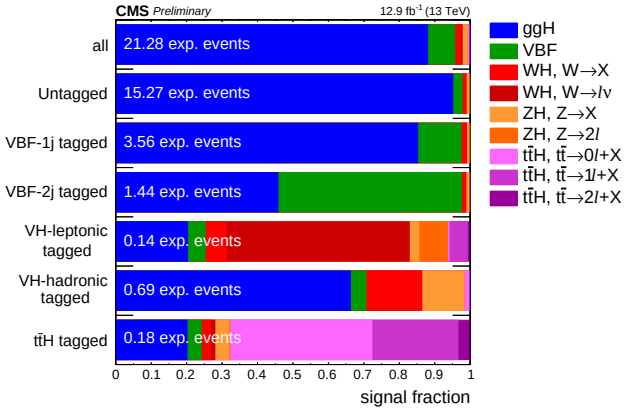

Figure 1: Signal relative purity of the six event categories in terms of the 5 main production mechanisms of the H(125) boson in a $118 < m_{4\ell} < 130$ GeV window. The WH, ZH and tt̄H processes are split according to the decay of associated objects, whereby X denotes anything else than a lepton.

selection of misidentified or secondary leptons are collectively denoted as Z+X and estimated by two independent methods using separate control samples in data.

3. Results

The inclusive distribution of the reconstructed four-lepton invariant mass $m_{4\ell}$ after event selection is shown in Fig. 2 (left) for the sum of the 4e, 4μ and $2e2\mu$ final states. The observed distribution agrees with the sum of signal and background expectations within the statistical uncertainties over the whole mass spectrum. Figure 2 (right) shows the joint distribution of the decay discriminant $\mathscr{D}^{\rm kin}_{\rm bkg}$ and $m_{4\ell}$ in the low-mass region, including information on the final states and categories of observed events.

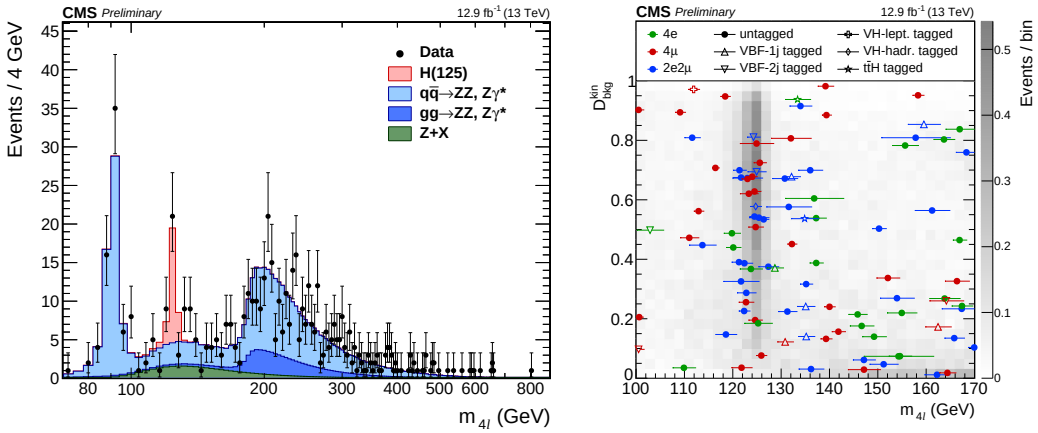

Figure 2: (left) Distribution of the four-lepton reconstructed invariant mass $m_{4\ell}$ in the full mass range. Points with statistical uncertainty bars represent the data and stacked histograms represent expected distributions. No events are observed with $m_{4\ell} > 850$ GeV. (right) Distribution of the kinematic discriminant $\mathscr{D}^{\rm kin}_{\rm bkg}$ versus $m_{4\ell}$ in the low-mass range. The gray scale represents the expected relative density of ZZ background plus H(125) signal. Points show the data, with per-event mass uncertainties shown as horizontal bars.

3.1 Significance and signal strength measurement

The significance of the excess of events observed near 125 GeV and the signal strength are measured via an unbinned two-dimensional maximum likelihood fit that exploits the $m_{4\ell}$ and $\mathscr{D}_{\rm bkg}^{\rm kin}$ observables. The distributions of selected events are split into 18 categories based on the six event categories and the three final states (4e, 4μ, 2e2μ).

Figure 3 (left) shows the significance of the local fluctuation with respect to the SM background-only expectation as a function of $m_{\rm H}$. The minimum of the local p-value is reached at 124.3 GeV and corresponds to a local significance of 6.4σ, while 6.3σ are expected for the SM Higgs boson. At the mass of $m_{\rm H} = 125.09$ GeV corresponding to the Run I combined LHC measurement, the observed (expected) significance is 6.2σ (6.5σ).

The signal strength μ is defined as the measured production cross section times branching fraction to four leptons divided by the SM expectation. At $m_{\rm H} = 125.09$ GeV, the simultaneous fit to all categories, profiling the likelihood for all nuisance parameters, leads to a value of $\mu = 0.99^{+0.33}_{-0.26}$. Two signal-strength modifiers $\mu_{\rm ggH,t\bar{t}H}$ and $\mu_{\rm VBF,VH}$ are then introduced as scale factors for the fermion and vector-boson induced contribution to the expected SM cross section, and are measured as $\mu_{\rm ggH,t\bar{t}H} = 1.00^{+0.39}_{-0.32}$ and $\mu_{\rm VBF,VH} = 0.91^{+1.56}_{-0.91}$ at the same mass. The 68% and 95% CL contours in the $(\mu_{\rm ggH,t\bar{t}H}, \mu_{\rm VBF,VH})$ plane are shown in Fig. 3 (center). Finally, four signal-strength modifiers $\mu_{\rm ggH}$, $\mu_{\rm VBF}$, $\mu_{\rm VH}$ and $\mu_{\rm t\bar{t}H}$, controlling the contributions of the main Higgs production modes, are constrained for the first time in the 4ℓ channel. The results are reported in Fig. 3 (right) and compared to the measured inclusive signal strength. All observed values are consistent with 1 within the uncertainties, which are dominated by the statistical ones with the current data set.

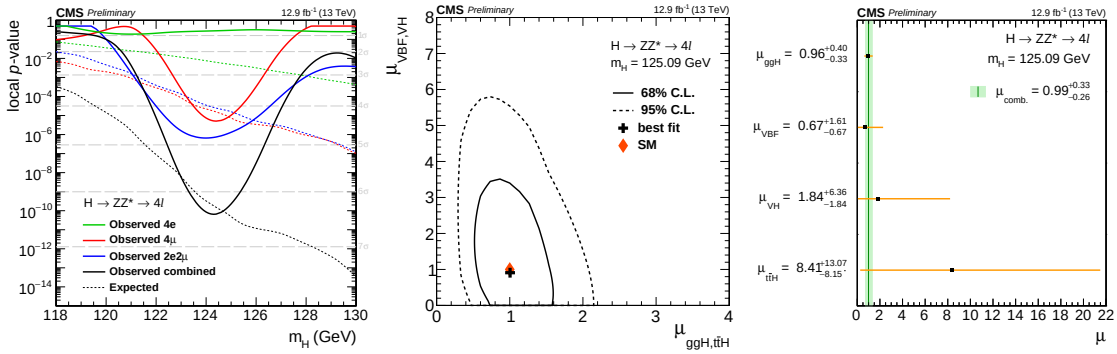

Figure 3: (left) p-value and significance of the local fluctuation with respect to the SM expectation as a function of $m_{\rm H}$. Dashed lines show the median expected p-values for the local mass hypothesis. (center) Result of the 2D likelihood scan for the $\mu_{\rm ggH,t\bar{t}H}$ and $\mu_{\rm VBF,VH}$ signal-strength modifiers. The solid and dashed contours show the 68% and 95% CL regions, the cross indicates the best-fit values, and the diamond shows the expected values for the SM Higgs boson. (right) Results of likelihood scans for the $\mu_{\rm ggH}$, $\mu_{\rm VBF}$, $\mu_{\rm VH}$ and $\mu_{\rm t\bar{t}H}$ signal-strength modifiers, with the combined μ shown as a vertical line. The horizontal bars and the filled band indicate the $\pm1\sigma$ uncertainties. All uncertainties include statistical and systematic sources.

3.2 Mass measurement

The measurement of the mass of the rediscovered Higgs boson exploits additional information from per-event relative mass uncertainties $\mathscr{D}_{\rm mass}$, which are defined by propagating per-lepton momentum errors to the 4ℓ candidate. Using this variable brings an expected improvement of about

8% to the uncertainty of the mass measurement, while the impact of also including $\mathscr{D}_{\rm bkg}^{\rm kin}$ is about 3%. Likelihood scans vs. $m_{\rm H}$ are shown in Fig. 4 (left) for a 1D fit (using only $m_{4\ell}$), a 2D fit ($m_{4\ell}$ and $\mathscr{D}_{\rm mass}$), and a 3D fit ($m_{4\ell}$, $\mathscr{D}_{\rm mass}$, and $\mathscr{D}_{\rm bkg}^{\rm kin}$). The signal strength μ is profiled, along with all nuisance parameters. The nominal result is given the 3D fit:

$$m_{\rm H} = 124.50^{+0.48}_{-0.46}\ {\rm GeV} = 124.50^{+0.47}_{-0.45}({\rm stat.})^{+0.13}_{-0.11}({\rm sys.})\ {\rm GeV}\ .$$

Figure 4 (right) presents the likelihood scan separately for the three final states.

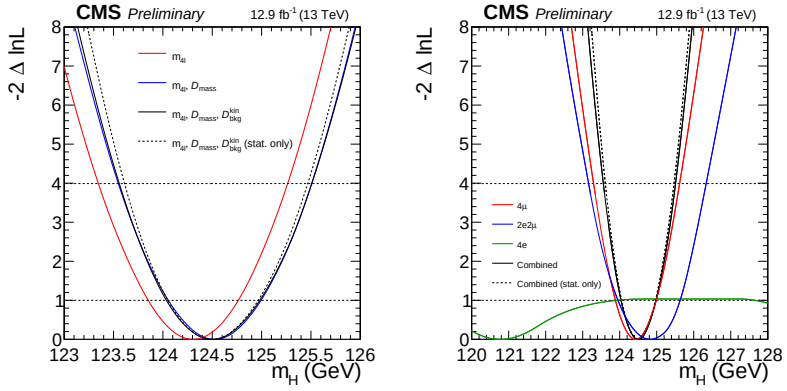

Figure 4: Likelihood scans versus $m_{\rm H}$, comparing the 1D, 2D, and 3D measurement (left), and showing the 3D measurement for the 3 final states and their combination (right). Solid lines represent scans with the full uncertainties from statistical and systematic sources, while dashed lines only include statistical uncertainties.

3.3 Fiducial cross section measurement

The fiducial cross section $\sigma_{\rm fid}$ for $pp \to H \to 4\ell$ is extracted from a maximum likelihood fit of signal and background parametrizations to the observed $m_{4\ell}$ distribution. The fiducial volume is defined as in Ref. [5]. The fit is performed simultaneously in all final states, assuming $m_{\rm H} = 125.0$ GeV and allowing branching ratios to different final states to float. Systematic uncertainties are included as nuisance parameters and effectively integrated out in the fit procedure. The number $N^i_{\rm obs}(m_{4\ell})$ of expected events in a given bin i of a considered observable is expressed as:

$$N^i_{\rm obs}(m_{4\ell}) = \varepsilon_{i,j}\cdot\left(1+f^i_{\rm nonfid}\right)\cdot\sigma^j_{\rm fid}\cdot\mathscr{L}\cdot\mathscr{P}_{\rm res}(m_{4\ell}) + N^i_{\rm nonres}\cdot\mathscr{P}_{\rm nonres}(m_{4\ell}) + N^i_{\rm bkg}\cdot\mathscr{P}_{\rm bkg}(m_{4\ell})\ .$$

The shape $\mathscr{P}_{\rm res}(m_{4\ell})$ of the resonant signal contribution is described by a double-sided Crystal Ball function, while the shape $\mathscr{P}_{\rm nonres}(m_{4\ell})$ of the non-resonant signal, which arises from VH and $t\bar{t}H$ events where a lepton from the $H \to 4\ell$ decay is not selected, is modeled by a Landau distribution and treated as a background. The detector response matrix $\varepsilon_{i,j}$, which maps numbers of expected events at the fiducial and reconstruction levels, is measured from simulation and corrected for residual differences between data and simulation. The shape of the contribution of reconstructed events that do not originate from the fiducial volume is verified to be identical to that of the fiducial signal, and its normalization is fixed to be a fraction $f_{\rm nonfid}$ of the latter. The value of $f_{\rm nonfid}$ is determined from simulation for each studied signal process. The model dependence of the measurement is determined by repeating the unfolding procedure while varying the relative fraction of each production mode within its experimental constraints. The integrated fiducial cross section is measured to be:

$$\sigma_{\rm fid} = 2.29^{+0.74}_{-0.64}({\rm stat.})^{+0.30}_{-0.23}({\rm sys.})^{+0.01}_{-0.05}({\rm model\ dep.})\ {\rm fb}\ ,$$

which can be compared to the SM expectation of $\sigma_{\text{fid}}^{\text{SM}} = 2.53 \pm 0.13$ fb. Figure 5 shows σ_{fid} as a function of $\sqrt{s}$, as well as results for every final state, and differential measurements as a function of the p_{T} of the Higgs boson and the number of selected jets.

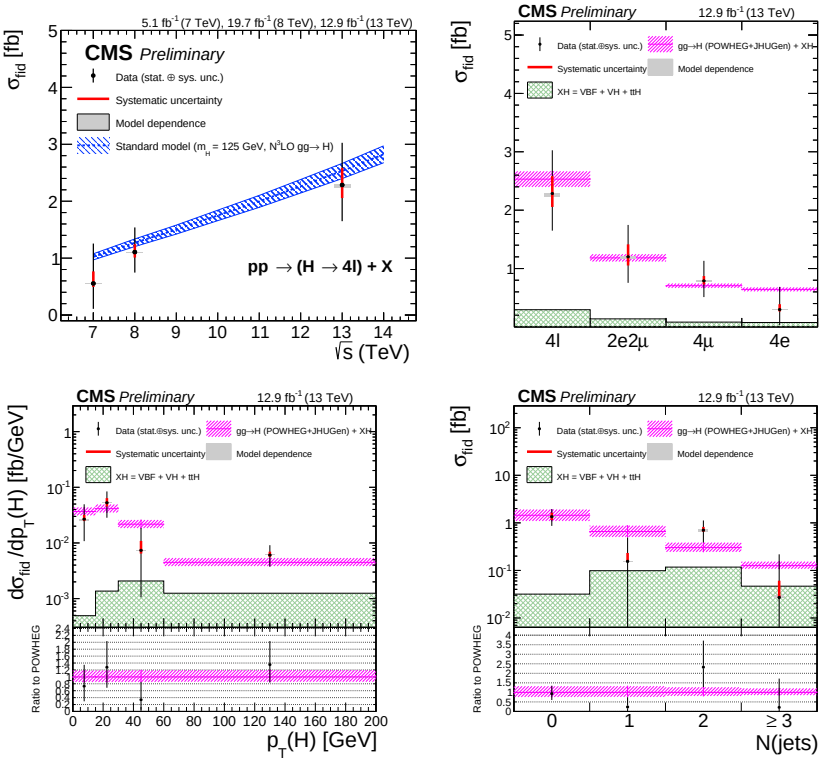

Figure 5: (top left) Measured fiducial cross section as a function of $\sqrt{s}$. (top right) Measured fiducial cross section in each final state. The subdominant component of the signal ($\text{VBF} + \text{VH} + \text{t}\bar{\text{t}}\text{H}$) is denoted as XH. (bottom) Measured differential cross section measurement as a function of $p_{\text{T}}(\text{H})$ (left) and N(jets) (right).

References

[1] ATLAS and CMS Collaborations, *Measurements of the Higgs boson production and decay rates and constraints on its couplings from a combined ATLAS and CMS analysis of the LHC pp collision data at* $\sqrt{s} = 7$ *and* 8 *TeV*, *JHEP* **08** (2016) 045

[2] ATLAS and CMS Collaborations, *Combined Measurement of the Higgs Boson Mass in pp Collisions at* $\sqrt{s} = 7$ *and* 8 *TeV with the ATLAS and CMS Experiments*, *Phys. Rev. Lett.* **114** (2015) 191803

[3] CMS Collaboration, *Measurement of the properties of a Higgs boson in the four-lepton final state*, *Phys. Rev. D* **89** (2014), 092007

[4] CMS Collaboration, *Measurement of differential and integrated fiducial cross sections for Higgs boson production in the four-lepton decay channel in pp collisions at* $\sqrt{s} = 7$ *and* 8 *TeV*, *JHEP* **04** (2016) 005

[5] CMS Collaboration, *Studies of Higgs boson production in the four-lepton final state at* $\sqrt{s} = 13$ *TeV*, CMS-PAS-HIG-15-004 (2016).

[6] CMS Collaboration, *Measurements of properties of the Higgs boson and search for an additional resonance in the four-lepton final state at* $\sqrt{s} = 13$ *TeV*, CMS-PAS-HIG-16-033 (2016).